ACS OMEGA

http://pubs.acs.org/journal/acsodf

Article

Power Generation by a Limestone-Contained Putty

Moon-Hyung Jang, Sean P. Rabbitte, Yu Lei, Simon Chung, and Gang Wang*

Cite This: *ACS Omega* 2023, 8, 9326–9333

Read Online

ACCESS | Metrics & More | Article Recommendations | Supporting Information

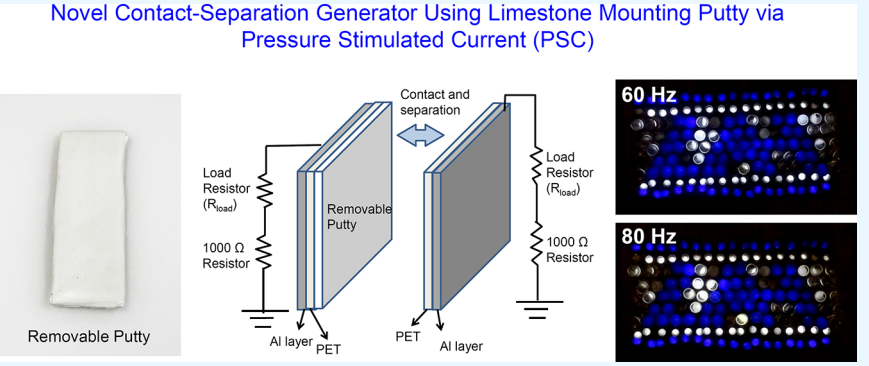

ABSTRACT: A novel contact−separation triboelectric generator concept is proposed in this paper, which consists of a limestone-based mounting putty and a metallized polyester (PET/Al) sheet. This is an attempt to explore tacky materials for power generation and extend the operational frequency bandwidth compared to existing TriboElectric NanoGenerators (TENGs). Moreover, the proposed design is very cost-effective and easy to build. Unlike traditional TENGs, which generate power solely due to a charge developing on the surface, the putty also replies on charge developed inside the material. Parametric study was conducted to determine the optimal putty thickness in a shaker test at 40 Hz. It was found that a putty layer at 0.6 mm thick yielded maximum power generation. During the separation phase, the electrical breakdown between triboelectric layers allows most existing electrons to flow back from the ground due to rapid charge removal at the interface. We are able to achieve a peak power of 16 mW in a shaker test at 40 Hz with an electrical load of 8 MΩ, which corresponds to a power density of 25.6 W/m^2. A peak power of 120 mW in a manual prototype generator is achieved, which operates at approximately 2 Hz. Since putty material has less tackiness than double-sided tape, we are able to expand the frequency bandwidth up to 80 Hz, which is significantly higher than a TENG (typically <10 Hz). The mounting putty material contains limestone with approximate 31 nm of mean grain size mixed with synthetic rubber materials. Elasticity from rubber and the nanohardness of calcite crystallites allow us to operate a putty generator repeatedly without the concern of grain fracture. Also, a durability test was conducted with up to 250,000 contact−separation cycles. In summary, comparable performance is achieved in the proposed putty generator to benefit energy harvesting and sensor applications.

INTRODUCTION

Since its invention in 2012, the TriboElectric Nanogenerator (TENG) has been extensively investigated by many scientists and researchers because it has a great potential to power low-power profile sensors and electronics in many engineering applications without a major impact on environments.[1−9] However, there are some challenges to overcome, primarily in improving performance. In addition, spark generation during the separation significantly reduces the efficiency of power generation.[10−13] Therefore, external pumping devices and circuits must be introduced in TENGs, which add the complexity of the system. For example, in one study, voltage multiplying circuits (VMCs) were used to increase the output voltage.[14] The maximum power density of 38.2 W/m^2 was obtained at a load resistance of 4 MΩ, which operates at 4 Hz. A power density of 40 W/m^2 was achieved when using a ferroelectric P(VDF-TrFE) triboelectric layer and a VMC circuit.[14] TENG with an external charge excitation module was established with a carbon/silicone gel electrode to avoid the air breakdown between triboelectric layers.[10] The power density at 115.6 W/m^2 was reported. Although recent TENG developments show enhanced performance in terms of power generation, the design and production of contact−separation-based TENGs must be simplified to reduce the system complexity and the environmental impact due to the involved chemical evaporation process during the fabrication.

Received: December 1, 2022
Accepted: February 21, 2023
Published: March 2, 2023

Recently, we proposed a new way of fabricating triboelectric generators by exploring tacky materials.[15] A simple configuration of an assembly with double-sided tape and PET/Al sheets allows us to obtain a peak power of 25 mW in a shaker test at 20 Hz, which corresponds to a power density of 20.4 W/m^2. The highest peak power is 106 mW in a manually operated prototype, which corresponds to a power density of 169.6 W/m^2. Compared to existing TENGs, which often use nanotechnology-based fabrication methods, this newly proposed triboelectric generator concept uses double-sided tape, making it far more cost-effective and simpler to build. The strong bonding nature of acrylic adhesive on the tape enables a higher charge when contact. In addition, the electric breakdown at the interface makes the most existing electrons to flow back to the ground during the separation, which contributes to additional power generation. The strong tackiness of a double-sided tape prevents from operating at higher frequencies. Small energy harvesting applications such as health monitoring and wearable exoskeleton systems require a wider frequency bandwidth to harvest the energy from human motion.[16−18] Therefore, it is necessary to explore less tacky materials for higher-frequency power generation.

In this paper, we propose a contact−separation triboelectric generator concept with a higher-frequency operation and design flexibility, which consists of a less tacky mounting putty material and a metallized polyester (PET/Al) sheet. Commercial off-the-shelf (COT) removable mount putty is typically made by limestone mixed with rubber polymer materials. The physical phenomenon of this putty-based triboelectric generator is different during contact phase. Instead of surface charge generation on the interface between triboelectric layers as observed in TENGs[1−9] and the double-sided tape-based triboelectric generator,[15] a removable mounting putty-based triboelectric generator produces charge inside the putty body. Therefore, the thickness of a putty layer plays a major role for maximum power generation. In geoscience, it is well known that minerals like limestone, marble, and sandstone have anomalous current generation when applying pressure to minerals due to a process known as pressure-stimulated current (PSC).[15,19−21] It has been proposed that PSC occurs because of a plastic deformation in minerals. Once PSC signal is observed, tested minerals were broken into pieces. In a limestone-concentrated putty material, the flexible nature of the putty allows power generation to be repeatable without any material failure due to applied pressure. The generated power depends on the thickness of the putty, which indicates that the contribution of the putty bulk material is crucial for a power generation. Similar to the double-sided tape-based triboelectric generator during the separation phase, the electrical breakdown between triboelectric layers allows most existing electrons to flow back from the ground due to rapid charge removal at the interface, which provides additional power output compared to TENGs.

A double-electrode configuration was adopted with an assembly of Al/PET−putty−PET/Al to achieve maximum power generation during contact-separation. Parametric study was conducted to determine the optimal putty layer thickness during a shaker test at 40 Hz. A putty layer with 0.6 mm thickness produced maximum power generation. A peak power of 16 mW was achieved in a shaker test at 40 Hz with an electrical load of 8 MΩ, which corresponds to a power density of 25.6 W/m^2. We can also evaluate the proposed putty-based triboelectric generator up to 80 Hz in a shaker test. A durability test was conducted up to 250,000 contact−separation cycles. It is shown that the performance of power generation degrades slightly. A manual putty triboelectric generator produces a peak power of 120 mW operating approximately at 2 Hz.

In summary, this newly proposed putty-based triboelectric generator was comprehensively evaluated. We are able to produce a comparable amount of power to the double-sided tape generator and TENGs with much higher frequency.

EXPERIMENTAL SETUP

A commercial off-the-shelf (COT) scotch removable mounting putty was selected, which is made by 3M Company. As shown in the safety data sheet, it contains limestone at 50−60 wt % and other ingredients such as TiO_2, polyolefin, and rubber with less than 10 wt %. Powder X-ray diffraction (XRD) was performed using a Rigaku Miniflex benchtop X-ray diffraction instrument at a wavelength of 1.5406 Å (Cu Kα) as shown in Figure 1. A metallized PET sheet (PET/Al) was employed to

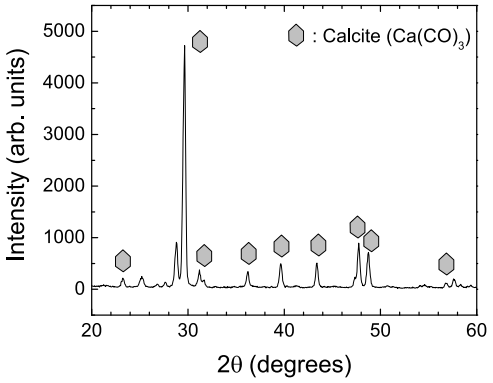

Figure 1. Powder X-ray diffraction (XRD) data of mounting putty. Peaks from calcite crystal ($Ca(CO)_3$) were assigned with gray hexagons.

serve as one triboelectric layer, which has a thickness of 50.8 μm (McMaster-Carr). The limestone-concentrated putty layer was interfaced with the PET side, and the Al layer served as the electrode. As aforementioned, a double-electrode design was adopted so that the putty layer is sandwiched between two PET/Al sheets as shown in Figure 2a. To produce a contact−separation motion, a Smart Shaker 2007E01 (The Modal Shop, Inc.) was used to drive the assembly sinusoidally ranging from 20 to 80 Hz. One PET/Al sheet is fixed to an Al framing, while putty/PET/Al was held on the Al block, which is attached to the shaker as shown in Figure 2b. The active contact area was 25 mm by 25 mm. A force sensor 208C01 (PCB Piezotronics) was attached between the shaker and the Al block to perform the force measurements during the contact−separation. Electrical wirings from Al to the circuit were configured with regular alligator clips. Power measurements were taken with a 1008A 8 channel USB digital oscilloscope (Hantek). Instead of measuring open circuit voltage (V_{OC}) and short circuit current (I_{SC}), the actual voltage and current values in a circuit were measured for better estimation of the power as shown in Figure 2a. Typically, voltage amplitudes ($V_{circuit}$) of load resistors were measured in channel 1. Voltage amplitudes ($V_{1000\,\Omega}$) of a 1000 Ω resistor connected in series were also performed in channel 2 to calculate the current ($I_{circuit}$) flow along the circuit by Ohm's law ($I_{circuit} = I_{1000\,\Omega} = V_{1000\,\Omega}/1000\ \Omega$). Then, the available

https://doi.org/10.1021/acsomega.2c07688
ACS Omega 2023, 8, 9326−9333

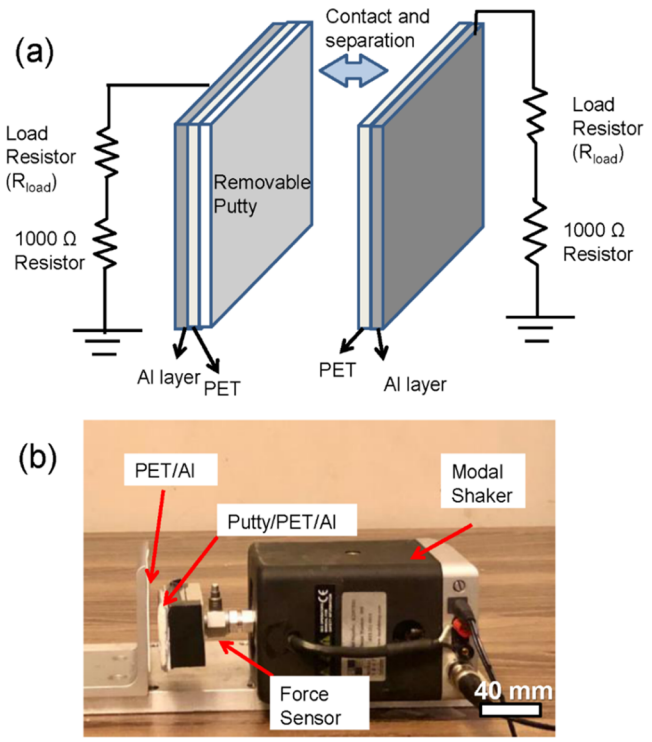

Figure 2. (a) Schematic of a putty generator with a double-electrode configuration. A load resistor of 1000 Ω resistor connected in series on both circuits to measure the voltage amplitude and current values separately and (b) shaker test setup of a putty generator with the Al/PET−putty−PET/Al configuration.

harvested power can be derived by calculating the product of $V_{circuit}$ and $I_{circuit}$. Channel 3 was used for the force sensor. Channels 4 and 5 were used for voltage and current measurements for calculating the harvested power from the other PET/Al sheet (i.e., Al/PET/putty−PET/Al combinations). A manual power generator with Al/PET/putty−PET/Al combinations was prepared as shown in Figure 10a. Polypropylene layers at four corners of the device were used as springs. The associated voltage and current measurement were performed as used in the shaker test.

RESULTS AND DISCUSSION

The powder XRD pattern of the mounting putty is shown in Figure 1. Calcite ($CaCO_3$) rhombohedral crystal peaks from limestone are identified in the plot.[22,23] Based on the Scherrer equation, the mean size of calcite grain can be estimated using the following equation

$$\tau = \frac{K\lambda}{\beta \cos\theta}$$

Here, K, λ, β, and θ are the shape factor, X-ray wavelength (Cu Kα: 1.5406 Å), the line broadening at FWHM (0.3°), and the Bragg angle (14.8°), respectively. The mean size of the calcite grain is found to be 31 nm by applying the above equation. Therefore, it is plausible to state that the greater portion of the limestone putty consists of calcite nanocrystallites.

To investigate the effect of putty thickness on the power generation, parametric studies were conducted by varying the putty thickness in a shaker test. Shaker putty generator with a double-electrode configuration (Al/PET/putty−PET/Al) is shown in Figure 2a. The input frequency was set at 40 Hz. A 4 MΩ resistor was introduced to serve as an electric load in the circuit. Figures 3a and 4a show voltage and current time history collected from the right Al electrode (PET/AL, shown in red) and left Al electrode (Al/PET/putty, shown in black), in which the putty thickness is 0.6 mm. Identical voltage and current profiles in the opposite phase are observed in both Al electrodes. Combined power history is shown in Figure 5a. An instantaneous peak power of 10 mW is achieved, which corresponds to a power density of 16 W/m^2. The power density value was slightly lower than our previous double-sided triboelectric generator15 (17.3 W/m^2 at 20 Hz). Nevertheless, the removable mounting putty has less tackiness compared to a double-sided tape, which enables it to use for higher-frequency power generation. The collected voltage time history for the case of 1.2 and 1.8 mm putty thicknesses is shown in Figure 3b,c, respectively. The associated current time history is shown in Figure 4b,c. A similar trend is obtained for both voltage and current as shown in Figures 3a and 4a when the putty thickness is 0.6 mm. However, there is a reduction on both voltage and current amplitude as the putty thickness increases. The corresponding power time history is shown in Figure 5b,c. Apparently, as the putty thickness increases, the power value decreases. This confirms that the charge generation depends on the thickness of putty in our putty-based triboelectric generator design. Figure 6 shows the effect of putty thickness on power generation. Note that the combined peak power value from both electrodes is plotted. The maximum power is observed when the putty thickness is 0.6 mm. As the thickness increases from 0.6 mm, the peak power drops and levels off at a constant value.

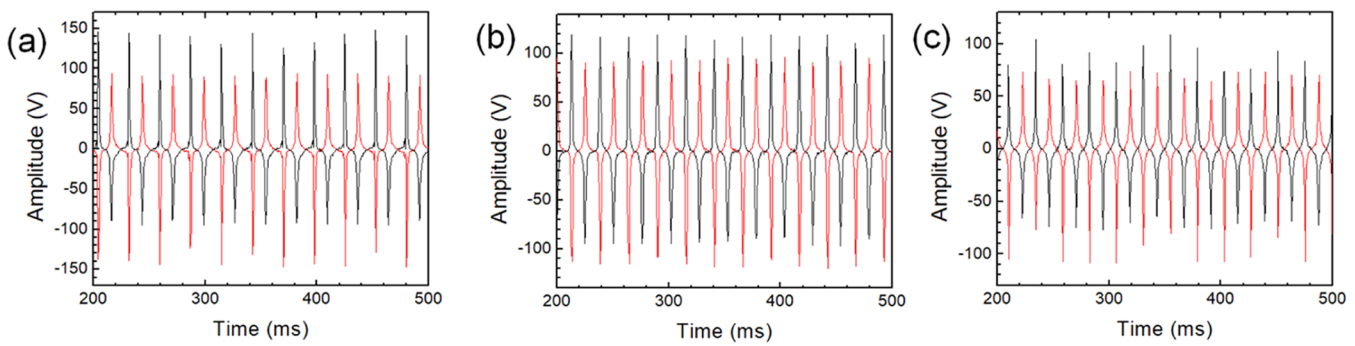

Figure 3. Putty thickness effect on the collected voltage: (a) 0.6 mm, (b) 1.2 mm, and (c) 1.8 mm (left Al electrode in black and right Al electrode in red).

https://doi.org/10.1021/acsomega.2c07688
ACS Omega 2023, 8, 9326−9333

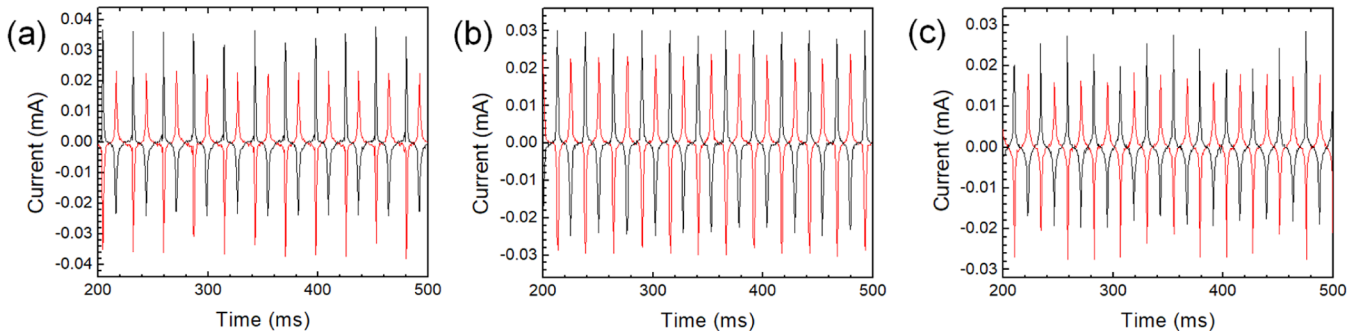

Figure 4. Putty thickness effect on the collected current: (a) 0.6 mm, (b) 1.2 mm, and (c) 1.8 mm (left Al electrode in black and right Al electrode in red).

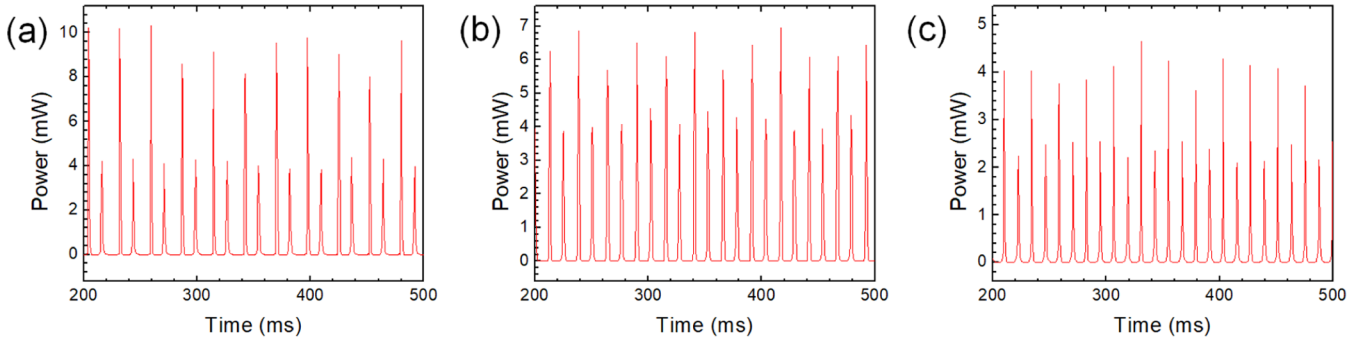

Figure 5. Putty thickness effect on instantaneous power: (a) 0.6 mm, (b) 1.2 mm, and (c) 1.8 mm (4 MΩ resistor served as an electrical load).

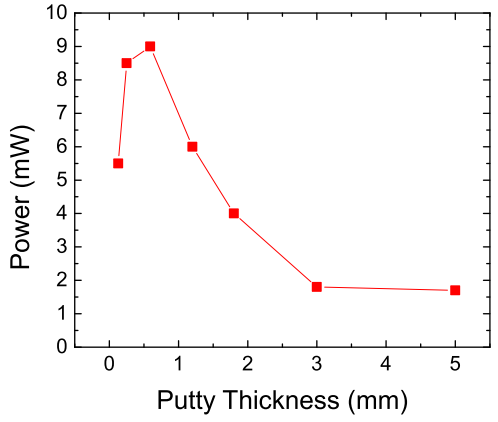

Figure 6. Average peak power as a function of putty thickness with an electrical load of 8 MΩ.

If we assume that the power generation is solely contributed by the triboelectric effect, when the putty layer becomes thicker, the distance between the putty and left Al electrode becomes too far for charge attraction. The power production from the putty side (i.e., $P = I_{\text{putty side}}{}^2 R_{\text{load}}$) will be negligible because the charge flow ($I = \mathrm{d}Q/\mathrm{d}t$) in the Al electrode is minimized. On the other hand, the right PET side will produce the same amount of electric field to the Al electrode since the charge is generated at the interface between putty and PET when contacting. Accordingly, the power generation will converge to half of the maximum value as the putty thickness increases. However, as shown in Figure 6, the peak power value varies with the putty thickness and does not converge to the expected half amount of peak value, which indicates that the assumption is not valid. Therefore, it is plausible that putty bulk plays an important role in power generation.

As a matter of fact, in geoscience, researchers observed an electric current emission with a positive voltage amplitude in some minerals including limestone when it was pressed.[20,21,24] It is called pressure-stimulated current (PSC). It was proposed that the plastic deformation (or fracture) of grains causes the electric pulse when limestone was pressed. Such a fracture would normally prevent limestone from being useful for a contact and separation-based energy harvesting operation. However, two reasons allow us to operate a putty generator repeatedly without the concern of grain fracture. First, the rubber contents introduce elasticity in a putty material. Second, once the crystallites of calcite become small as nanoscale sizes, i.e., diameter less than 200 nm, the nanohardness of the crystallites increases abruptly to 2.74 GPa compared to the Vickers hardness number of 105−135 (1.03−1.334 GPa).[25] Therefore, a substantial force is required to induce potential fracture damage in limestone minerals. It is observed that power generation depends on the applied pressure during contact. Less power generation is achieved when the contact pressure decreases.

Both 40 and 65.6 kPa were applied to our putty generator in a shaker test at 40 Hz. The peak power of 10 mW was observed when the pressure is 65.6 kPa, which is higher than the peak power value of 6 mW in the 40 kPa case. Not that those pressure values are nowhere close to the hardness value of the limestone whether it is in nanosize or not. Therefore, the limestone putty generator can be operated for a long period of time without material degradation concern. A durability test was performed and will be discussed in a later section.

As a rule of thumb, the electric field (E) on the left electrode can be expressed as $E = Q/(4\pi\varepsilon d^2)$ in terms of permittivity (ε), total charge generated in putty layer (Q), and mean distance (d). Namely, if the putty thickness increases, the attraction from generated charges will become weaker to cause a drop in

https://doi.org/10.1021/acsomega.2c07688
ACS Omega 2023, 8, 9326−9333

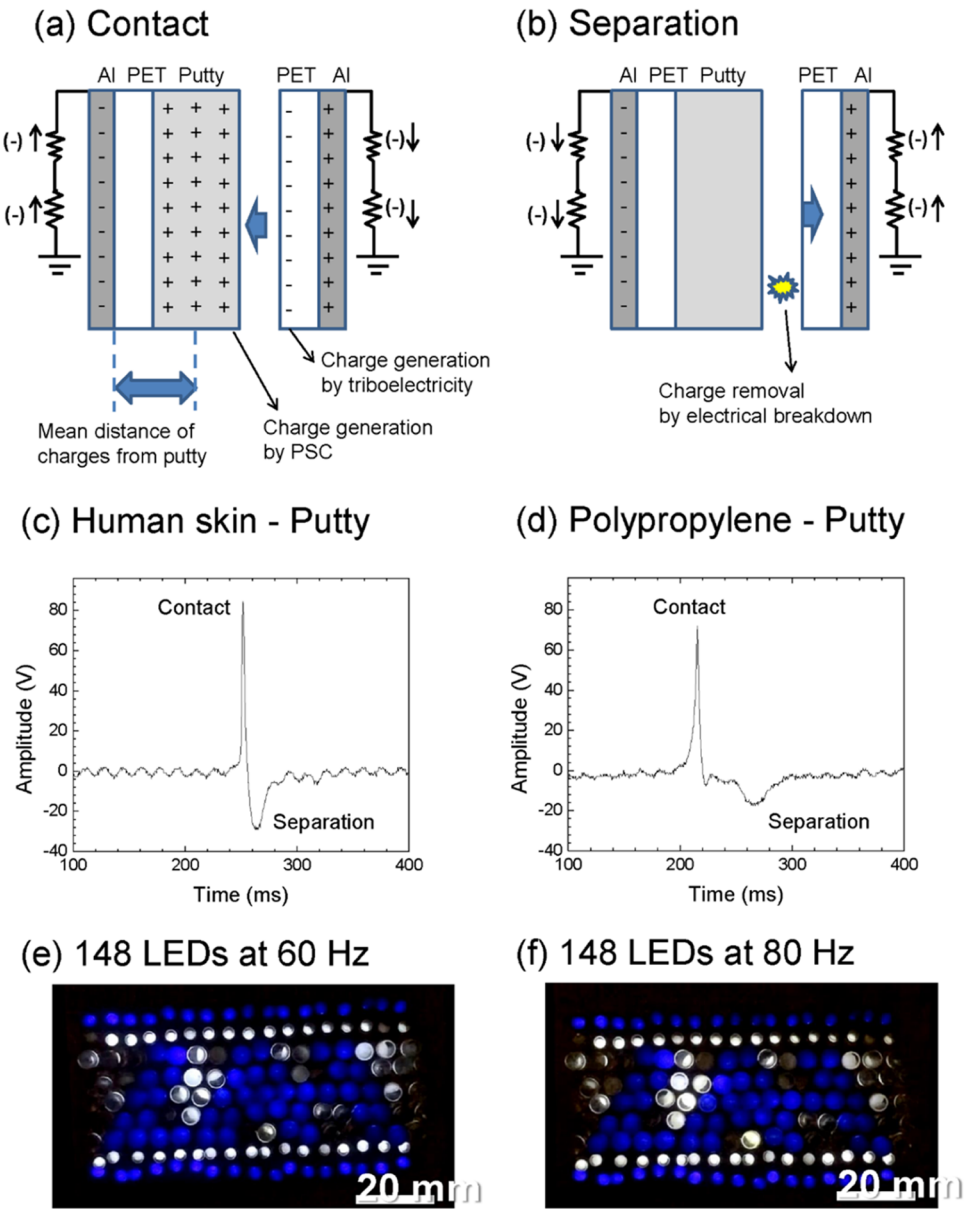

Figure 7. Schematics of the electric charge generation in a putty triboelectric generator in (a) a contact and (b) a separation, respectively. Panels (c) and (d) show open circuit voltage from putty when interfaced with human skin and polypropylene material in a tapping test, respectively. Panels (e) and (f) show LEDs lighting up at a high-frequency shaker operation at 60 and 80 Hz, respectively.

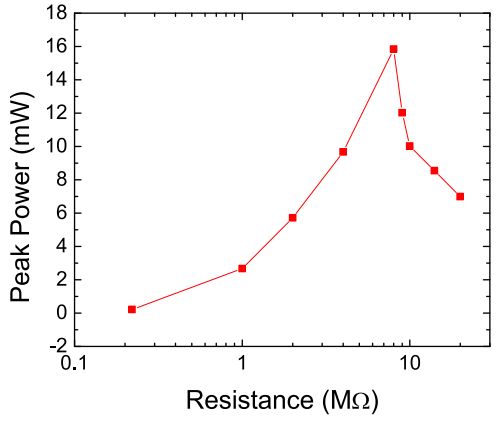

Figure 8. Peak power as a function of electric loads with a 0.6 mm putty thickness.

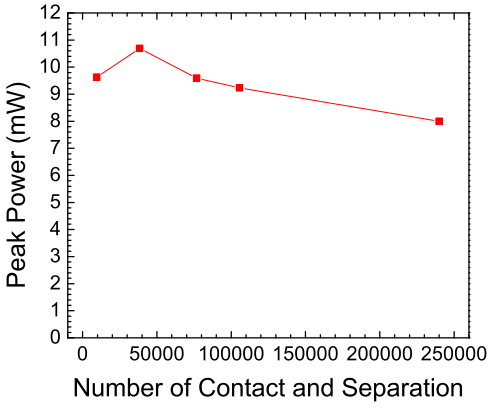

Figure 9. Durability test with a 0.6 mm putty thickness and a 4 MΩ electrical load as shown in Figure 2.

https://doi.org/10.1021/acsomega.2c07688
ACS Omega 2023, 8, 9326−9333

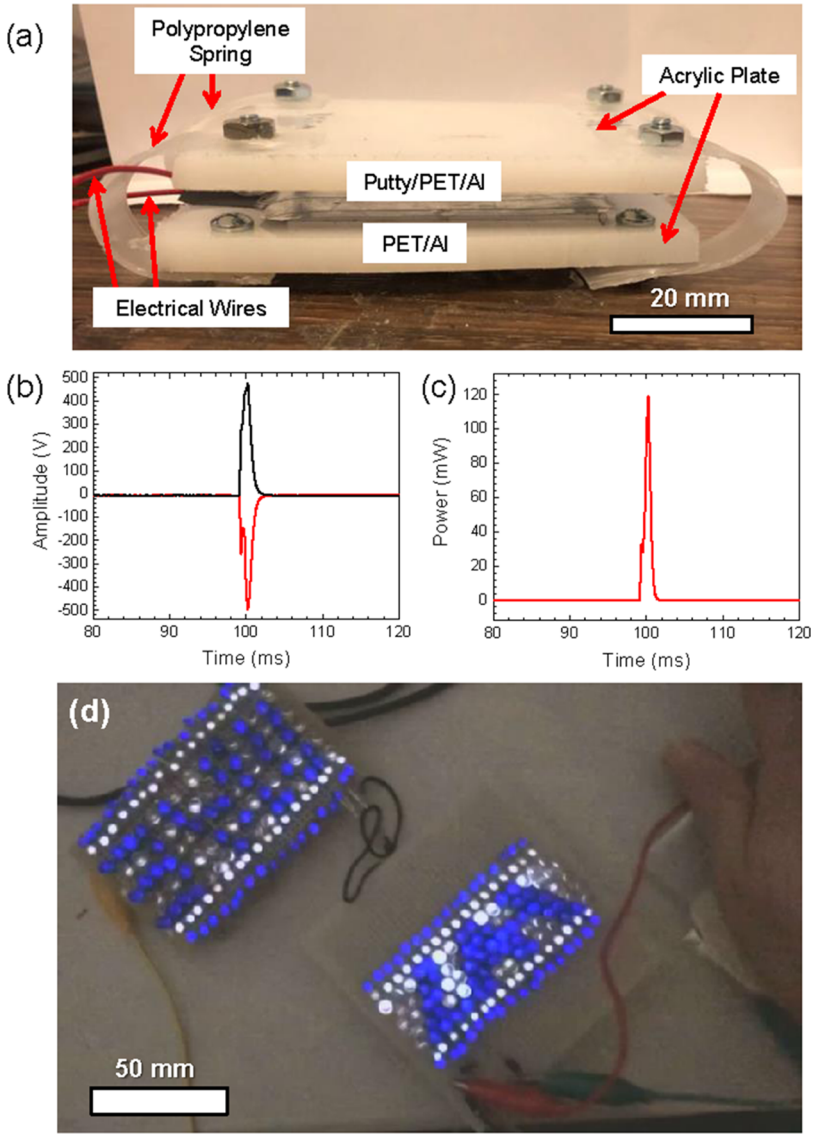

Figure 10. (a) Picture of a manual putty generator and assembly of Al/PET−putty−PET/Al attached to the top and bottom plastic plates and polypropylene springs on both sides; (b) voltage amplitudes of the top Al electrode (black) and bottom Al electrode (red); (c) combined power; and (d) 296 LEDs lighting on by the manual putty generator operation with a hand.

power generation. Also, a thicker putty will produce a less charge density per unit volume since total charge Q remains the same throughout the putty bulk under the same applied force. However, when the putty thickness is below 0.6 mm, the total charge Q generation is limited by a very thin layer of putty. Accordingly, the peak power decreases as shown in Figure 6.

Based on the above observation and discussion, the operational principle of a putty triboelectric generator is explained in Figure 7a,b. In contact as shown in Figure 7a, putty bulk generates positive charges throughout its thickness, while the PET layer generates negative charges only on its surface. Since the electron attraction in the Al electrode (left) inversely depends on the square of the mean distance between the Al electrode and putty, which is approximated by the PET thickness plus half of putty thickness, the power generation depends on the thickness of putty. On the right-hand side, negative charges in PET will attract positive charges in the Al electrode. In separation as shown in Figure 7b, the air breakdown removes all charges inside the putty and on the surface of a PET. The attracted charges in Al electrodes will flow back to the ground.

The behavior of the limestone putty in power generation is quite similar to the high entropy materials (HEMs).[26] For example, high entropy materials have a tendency to form nanotwins with lower stacking fault energy when the force is applied to the system.[27] This distortion of lattice is responsible for increasing the electron mean free path.[28] In limestone putty, PSC can be generated because of the plastic deformation of crystals under pressure. Therefore, it is plausible that the applied mechanical energy is possibly absorbed in a way of producing plastic deformations of limestone in putty. It may lead to increase the electron mean free path like HEMs so that PSC can be observed in the energy harvester.

To verify the charge generation by PSC instead of the triboelectric effect during a contact, a putty layer, which has a size of 25 mm × 25 mm × 1 mm, was interfaced with both human skin and polypropylene material in a tapping test, in which a Cu grid sheet is integrated inside the putty to serve as an electrode. Human skin and polypropylene are very strong

https://doi.org/10.1021/acsomega.2c07688
ACS Omega 2023, 8, 9326−9333

positive triboelectric materials with charge affinities of 45 and 55 nC/J, respectively.[29] If the charge is contributed by the triboelectric effect, a negative voltage will be collected during a contact since skin and polypropylene surfaces are strongly positive. If a positive voltage is observed during a contact, this indicates that positive charges are generated via PSC instead of triboelectrification. Figure 7c,d shows the collected open circuit voltage signals for human skin and polypropylene case, respectively. Positive voltage is clearly demonstrated in both cases when contacting. Moreover, almost the same peak voltage amplitude is observed in both cases, which indicates that PSC contributes to the charge developed inside the putty. Therefore, it is a direct proof that the limestone putty has a different way of generating electricity during a contact.

Figure 7e,f shows 148 LEDs lighting up using a putty triboelectric generator in a shaker test at 60 and 80 Hz, respectively (see Supporting Videos S1 and S2). It indicates that the limestone putty generator extends the operational frequency for broader applications.

Figure 8 shows the peak power as a function of electrical loads for the putty generator with the double-electrode configuration in a shaker test at 40 Hz, in which the putty thickness is 0.6 mm. Both voltage and current were measured separately from the Al electrode using the circuit as described in Figure 2a to derive the total harvested power. The combined highest peak power was 16 mW under an electrical load of 8 MΩ, which corresponds to the power density of 25.6 W/m^2.

As shown in Figure 9, a durability test was performed for our putty generator in a shaker test at 40 Hz, in which the putty thickness is 0.6 mm and a 4 MΩ electrical load is connected to both electrodes. The peak power starts with a value of 9.5 mW and slightly increases to 11 mW at 40,000 contact−separation cycles. Then, it decreases slightly to 8 mW at 250,000 cycles. It is shown that power generation degrades slightly. A manual putty generator is shown in Figure 10a with an assembly of Al/PET−putty−PET/Al attached to the top and bottom plastic plates, in which polypropylene materials are used for springs on both sides. The contact-separation motion can be introduced manually, which operates approximately at 2 Hz. The collected voltage from both Al electrodes and combined power are shown in Figure 10b,c, respectively. The peak power was 120 mW with an active area of 50 mm × 50 mm. The power density of the manual generator was 48 W/m^2. Therefore, the manual generator demonstrated higher power generation compared to the case in the shaker test because the polypropylene springs allow faster separation for quicker charge dissipation. A demonstration of a manual putty generator using 296 LEDs is shown in Figure 10d (see Supporting Video S3).

In summary, the proposed putty-based triboelectric generator shows comparable performance in contrast to existing TENGs and our previous double-sided tape triboelectric generator.[15] Moreover, less tackiness allows us to operate it at a higher frequency, which could lead to a new sensor design configuration.

CONCLUSIONS

In this paper, we proposed a putty-based triboelectric generator concept, which is composed of an assembly of Al/PET−putty−PET/Al. Power generation is comparable to the state of the art of TENG devices. Key conclusions are summarized below:

- This is the first attempt to utilize the mounting putty material in the triboelectric generator design.
- Under different putty thicknesses, power output changes since PSC generates charges inside putty bulk materials, which is different from surface charge generation as typically observed in TENGs.
- Putty generator has potential for use at high frequencies since it has less tackiness than a double-sided tape. We are able to extend the frequency bandwidth to 80 Hz, which is significantly higher than a TENG (typically <10 Hz).
- Current simple design allows easy fabrication with only a craft-level skill compared to the nanotechnology-based techniques used in TENG devices.

Further investigation on putty-based generators is expected to explore different minerals such as marble, sandstone, and lunar soil with abundant amounts of Ca in plagioclase. It is also important to fully understand the charging mechanism at small-scale levels.

ASSOCIATED CONTENT

Supporting Information

The Supporting Information is available free of charge at https://pubs.acs.org/doi/10.1021/acsomega.2c07688.

148 LEDs lighting up at 60 Hz of frequency by a putty generator with a modal shaker and a bridge rectifier (MP4)

148 LEDs lighting up at 80 Hz of frequency by a putty generator with a modal shaker and a bridge rectifier (MP4)

296 LEDs lighting up by a manual putty generator via contact-separation operations (MP4)

AUTHOR INFORMATION

Corresponding Author

Gang Wang − *Department of Mechanical and Aerospace Engineering, The University of Alabama in Huntsville, Huntsville, Alabama 35899, United States;* orcid.org/0000-0001-9843-5966; Email: gang.wang@uah.edu

Authors

Moon-Hyung Jang − *Department of Mechanical and Aerospace Engineering, The University of Alabama in Huntsville, Huntsville, Alabama 35899, United States; Department of Chemical and Materials Engineering, The University of Alabama in Huntsville, Huntsville, Alabama 35899, United States*

Sean P. Rabbitte − *Department of Mechanical and Aerospace Engineering, The University of Alabama in Huntsville, Huntsville, Alabama 35899, United States*

Yu Lei − *Department of Chemical and Materials Engineering, The University of Alabama in Huntsville, Huntsville, Alabama 35899, United States;* orcid.org/0000-0002-4161-5568

Simon Chung − *Materials Sciences LLC, Horsham, Pennsylvania 19044, United States*

Complete contact information is available at: https://pubs.acs.org/10.1021/acsomega.2c07688

Author Contributions

G.W. proposed the idea of using Al/PET sheet as a triboelectric layer. M.-H.J. proposed the idea of using putty

https://doi.org/10.1021/acsomega.2c07688
ACS Omega 2023, 8, 9326−9333

as another triboelectric layer. Shaker and manual triboelectric generator tests were performed by M.-H.J. and S.P.R. Manual generator design was proposed by M.-H.J. M.-H.J. analyzed the data. Results are discussed by M.-H.J., G.W., Y.L., and S.C. M.-H.J., G.W., and S.P.R. prepared the manuscript.

Notes

The authors declare no competing financial interest.

■ ACKNOWLEDGMENTS

This project was partially sponsored by the College of Engineering at the University of Alabama in Huntsville and Material Sciences LLC.

■ REFERENCES

(1) Wang, Y.; Yang, Y.; Wang, Z. L. Triboelectric nanogenerators as flexible power sources. *npj Flex. Electron.* **2017**, *1*, No. 10.
(2) Liu, W.; Wang, Z.; Wang, G.; Liu, G.; Chen, J.; Pu, X.; Xi, Y.; Wang, X.; Guo, H.; Hu, C.; Wang, Z. L. Integrated charge excitation triboelectric nanogenerator. *Nat. Commun.* **2019**, *10*, No. 1426.
(3) Tang, Q.; Yeh, M.-H.; Liu, G.; Li, S.; Chen, J.; Bai, Y.; Feng, L.; Lai, M.; Ho, K.-C.; Guo, H.; Hu, C. Whirligig-inspired triboelectric nanogenerator with ultrahigh specific output as reliable portable instant power supply for personal health monitoring devices. *Nano Energy* **2018**, *47*, 74−80.
(4) Zhu, G.; Pan, C.; Guo, W.; Chen, C.-Y.; Zhou, Y.; Yu, R.; Wang, Z. L. Triboelectric-Generator-Driven Pulse Electrodeposition for Micropatterning. *Nano Lett.* **2012**, *12*, 4960−4965.
(5) Huang, C.; Chen, G.; Nashalian, A.; Chen, J. Advances in self-powered chemical sensing via a triboelectric nanogenerator. *Nanoscale* **2021**, *13*, 2065−2081.
(6) Wang, H.; Xu, L.; Bai, Y.; Wang, Z. L. Pumping up the charge density of a triboelectric nanogenerator by charge-shuttling. *Nat. Commun.* **2020**, *11*, No. 4203.
(7) Wang, J.; Wu, C.; Dai, Y.; Zhao, Z.; Wang, A.; Zhang, T.; Wang, Z. L. Achieving ultrahigh triboelectric charge density for efficient energy harvesting. *Nat. Commun.* **2017**, *8*, No. 88.
(8) Dharmasena, R. D. I. G.; Silva, S. R. P. Towards optimized triboelectric nanogenerators. *Nano Energy* **2019**, *62*, 530−549.
(9) Fan, F.-R.; Tian, Z.-Q.; Lin Wang, Z. Flexible triboelectric generator. *Nano Energy* **2012**, *1*, 328−334.
(10) Liu, Y.; Liu, W.; Wang, Z.; He, W.; Tang, Q.; Xi, Y.; Wang, X.; Guo, H.; Hu, C. Quantifying contact status and the air-breakdown model of charge-excitation triboelectric nanogenerators to maximize charge density. *Nat. Commun.* **2020**, *11*, No. 1599.
(11) Cao, Z.; Chu, Y.; Wang, S.; Wu, Z.; Ding, R.; Ye, X. In *A Strategy to Reduce Air Breakdown Effect and Boost Output Energy for Contact-Separation Mode Triboelectric Nanogenerator*, 2021 21st International Conference on Solid-State Sensors, Actuators and Microsystems (Transducers), 2021; pp 451−454.
(12) Luo, J.; Xu, L.; Tang, W.; Jiang, T.; Fan, F. R.; Pang, Y.; Chen, L.; Zhang, Y.; Wang, Z. L. Direct-Current Triboelectric Nanogenerator Realized by Air Breakdown Induced Ionized Air Channel. *Adv. Energy Mater.* **2018**, *8*, No. 1800889.
(13) Liu, D.; Zhou, L.; Li, S.; Zhao, Z.; Yin, X.; Yi, Z.; Zhang, C.; Li, X.; Wang, J.; Wang, Z. L. Hugely Enhanced Output Power of Direct-Current Triboelectric Nanogenerators by Using Electrostatic Breakdown Effect. *Adv. Mater. Technol.* **2020**, *5*, No. 2000289.
(14) Li, Y.; Zhao, Z.; Liu, L.; Zhou, L.; Liu, D.; Li, S.; Chen, S.; Dai, Y.; Wang, J.; Wang, Z. L. Improved Output Performance of Triboelectric Nanogenerator by Fast Accumulation Process of Surface Charges. *Adv. Energy Mater.* **2021**, *11*, No. 2100050.
(15) Jang, M.-H.; Lee, J. D.; Lei, Y.; Chung, S.; Wang, G. Power Generation by a Double-Sided Tape. *ACS Omega* **2022**, *7*, 42359−42369.
(16) Gai, Y.; Wang, E.; Liu, M.; Xie, L.; Bai, Y.; Yang, Y.; Xue, J.; Qu, X.; Xi, Y.; Li, L.; et al. A Self-Powered Wearable Sensor for Continuous Wireless Sweat Monitoring. *Small Methods* **2022**, *6*, No. 2200653.
(17) Gai, Y.; Bai, Y.; Cao, Y.; Wang, E.; Xue, J.; Qu, X.; Liu, Z.; Luo, D.; Li, Z. A Gyroscope Nanogenerator with Frequency Up-Conversion Effect for Fitness and Energy Harvesting. *Small* **2022**, *18*, No. 2108091.
(18) Hu, B.; Xue, J.; Jiang, D.; Tan, P.; Wang, Y.; Liu, M.; Yu, H.; Zou, Y.; Li, Z. Wearable Exoskeleton System for Energy Harvesting and Angle Sensing Based on a Piezoelectric Cantilever Generator Array. *ACS Appl. Mater. Interfaces* **2022**, *14*, 36622−36632.
(19) Zhang, X.; Li, Z.; Wang, E.; Li, B.; Song, J.; Niu, Y. Experimental investigation of pressure stimulated currents and acoustic emissions from sandstone and gabbro samples subjected to multi-stage uniaxial loading. *Bull. Eng. Geol. Environ.* **2021**, *80*, 7683−7700.
(20) Enomoto, Y.; Hashimoto, H. Emission of charged particles from indentation fracture of rocks. *Nature* **1990**, *346*, 641−643.
(21) Agalianos, G.; Tzagkarakis, D.; Loukidis, A.; Pasiou, E. D.; Triantis, D.; Kourkoulis, S. K.; Stavrakas, I. Correlation of Acoustic Emissions and Pressure Stimulated Currents recorded in Alfas-stone specimens under three-point bending. The role of the specimens' porosity: Preliminary results. *Procedia Struct. Integr.* **2022**, *41*, 452−460.
(22) Graf, D. L. Crystallographic tables for the rhombohedral carbonates. *Am. Min.* **1961**, *46*, 1283−1316.
(23) Markgraf, S. A.; Reeder, R. J. High-temperature structure refinements of calcite and magnesite. *Am. Min.* **1985**, *70*, 590−600.
(24) Stavrakas, I.; Triantis, D.; Agioutantis, Z.; Maurigiannakis, S.; Saltas, V.; Vallianatos, F.; Clarke, M. Pressure stimulated currents in rocks and their correlation with mechanical properties. *Nat. Hazards Earth Syst. Sci.* **2004**, *4*, 563−567.
(25) Kabacińska, Z.; Yate, L.; Wencka, M.; Krzyminiewski, R.; Tadyszak, K.; Coy, E. Nanoscale Effects of Radiation (UV, X-ray, and γ) on Calcite Surfaces: Implications for its Mechanical and Physico-Chemical Properties. *J. Phys. Chem. C* **2017**, *121*, 13357−13369.
(26) Tsai, M.-H.; Yeh, J.-W. High-Entropy Alloys: A Critical Review. *Mater. Res. Lett.* **2014**, *2*, 107−123.
(27) Tang, Z.; Yuan, T.; Tsai, C.-W.; Yeh, J.-W.; Lundin, C. D.; Liaw, P. K. Fatigue behavior of a wrought Al0.5CoCrCuFeNi two-phase high-entropy alloy. *Acta Mater.* **2015**, *99*, 247−258.
(28) Chou, H.-P.; Chang, Y.-S.; Chen, S.-K.; Yeh, J.-W. Microstructure, thermophysical and electrical properties in AlxCoCrFeNi ($0 \le x \le 2$) high-entropy alloys. *Mater. Sci. Eng.: B* **2009**, *163*, 184−189.
(29) The Triboelectric Effect Series - AlphaLab. Inc.. https://www.alphalabinc.com/triboelectric-series/ (accessed Dec 12, 2022).

https://doi.org/10.1021/acsomega.2c07688
ACS Omega 2023, 8, 9326−9333